Journal of Molecular Liquids, 40 (1989) 251–260
Elsevier Science Publishers B.V., Amsterdam – Printed in The Netherlands

Birefringence Effects Induced by Optical Saturation, Dispersion Effects in the Far Infra-red.

M. W. Evans, * G. C. Lie, and E. Clementi

IBM Corporation
Data Systems Division
Dept. 48B / MS 428
Neighborhood Road
Kingston, New York 12401

(Received 11 January 1989)

*Permanent Address:
Department of Physics
University College of Swansea
Singleton Park
Swansea SA2 8PP, Wales (UK)
and
Visiting Academic
Dept. of Microelectronics & Electrical Engineering
Trinity College
Dublin 2, Republic of Ireland

Abstract

It has been demonstrated recently, using computer simulation, that a molecular liquid treated with strong electromagnetic radiation becomes birefringent in the far infra red region of the electromagnetic spectrum This appears to be a new observation, opening the way for the spectral investigation of molecular dynamics with powerful laser fields.It is shown in this paper that the birefringence is accompanied by dispersion at frequencies characteristic of the molecular dynamics on the picosecond time scale.Dispersion of the birefringence that accompanies dynamic optical saturation is a new practical method of investigating molecular material at far infra red frequencies.

0167-7322/89/$03.50

Introduction

The term "optical saturation" is usually applied to the physical dielectric and optical effects of a powerful laser field in condensed molecular matter.[1-5] The light intensity conveyed by a laser beam can be so great as to cause saturation. The ratio

$$\mu E/kT$$

goes to infinity, where E is the electric field component of the electromagnetic field, μ is the molecular dipole moment, k the Boltzmann constant and T the absolute temperature.There are also second order and higher order saturation effects induced by the same field.The laser beam reorientation occurs following a 3.0×10^{-8} giant ruby laser pulse of approx. 10^9 to 10^{10} V m^{-1}. Monitoring of the far infra red spectrum by interferometry[6] during the application of the pulse would enable the measurement of birefringence and dichroism in the axes mutually perpendicular to those of the electromagnetic field. Computer simulation is a convenient way of estimating numerically the extent of this birefringence as a function of the applied field frequency.This could be measured experimentally by varying the frequency of the giant ruby laser field while using fast detector time resolved far infra red interferometry[7] to measure the extent of the birefringence for each ruby laser frequency.The information obtained by a combination of numerical and experimental techniques in this way would be of interest in the investigation of non linear molecular dynamics in response to intense applied electromagnetic fields . In chiral molecules[8] there is the exta dimension of circular dichroism, which could be utilised for the analysis of the different response of enantiomer and racemic mixture.

Theoretical Background

The giant ruby laser field has a vector potential which may be written as

$$\mathbf{A} = Re\{A_0 \exp(i\mathbf{k}.\mathbf{r} - \omega t)\} \quad (1)$$

and related to the electric and magnetic field intensities by

$$\mathbf{E} = ik\mathbf{A} \quad (2)$$

$$\mathbf{H} = i\mathbf{k} \times \mathbf{A} \quad (3)$$

Here k is the wave vector, r a vector displacement in the direction in which the field is applied, ω the frequency of the laser field and t the time.The wave vector is defined by

$$\mathbf{k} = \frac{\omega}{c}\mathbf{n} \quad (4)$$

where n is a unit vector in the direction of propagation of the wave.If the field is circularly polarised it may be written as

$$E_y = \cos(\omega t - \mathbf{k}.\mathbf{r}) \quad (5)$$

$$E_x = \sin(\omega t - \mathbf{k}.\mathbf{r}) \quad (6)$$

and is termed left or right circularly polarised according to the sign in the second equation.

For electromagnetic radiation c is the speed of light, but for thermal neutrons this is replaced by the neutron beam velocity . The wave vector for neutron beam induced birefringence is thus much greater in magnitude than the equivalent for laser induced birefringence and in this case the factor

$$\mathbf{k}.\mathbf{r}$$

is not negligible with respect to

$$\omega t.$$

For laser induced birefringence the former is negligible compared with the latter for frequencies up to 10^{14}.The laser field equations can therefore be written as the circularly polarised electric field equations (5) and (6) in this approximation.

The magnetic component of the giant ruby laser field is related to the electric component through the wave vector, viz.:

$$\mathbf{H} = \frac{\mathbf{k}}{k} \times \mathbf{E} \tag{7}$$

and this means that the magnetic component as well as the electric component can produce birefringence in the far infra red region.

Electric Field Induced Birefringence

The electric field induced birefringence is induced via the torque generated between the electric field vector and the molecular dipole moment ω. Similarly there is a birefringence generated between the magnetic component of the electromagnetic field and the electric dipole moment

$$\mathbf{H} \times \mu = (\frac{\mathbf{k}}{k} \times \mathbf{E}) \times \mu \tag{8}$$

In this paper the effect of these torques is simulated using 108 water molecules and 6,000 time steps.

Computer Simulation Methods

The methods used to simulate the development of birefringence are based on the constant volume[10] algorithm TETRA.The thermal torques generated by intermolecular forces are supplemented by a torque due to the giant ruby laser pulse.The dynamical trajectories are then generated over a total of 6000 time steps of 0.5 fs each and used to evaluate the time correlation functions by running time averaging.The intermolecular pair potential for the energy between two water molecules is a five by five site site model based on Lennard Jones and partial charge terms as described fully elsewhere in the literature.Off-diagonal elements of the cross correlation tensors are generated with transposition and normalisation as described fully elsewhere.

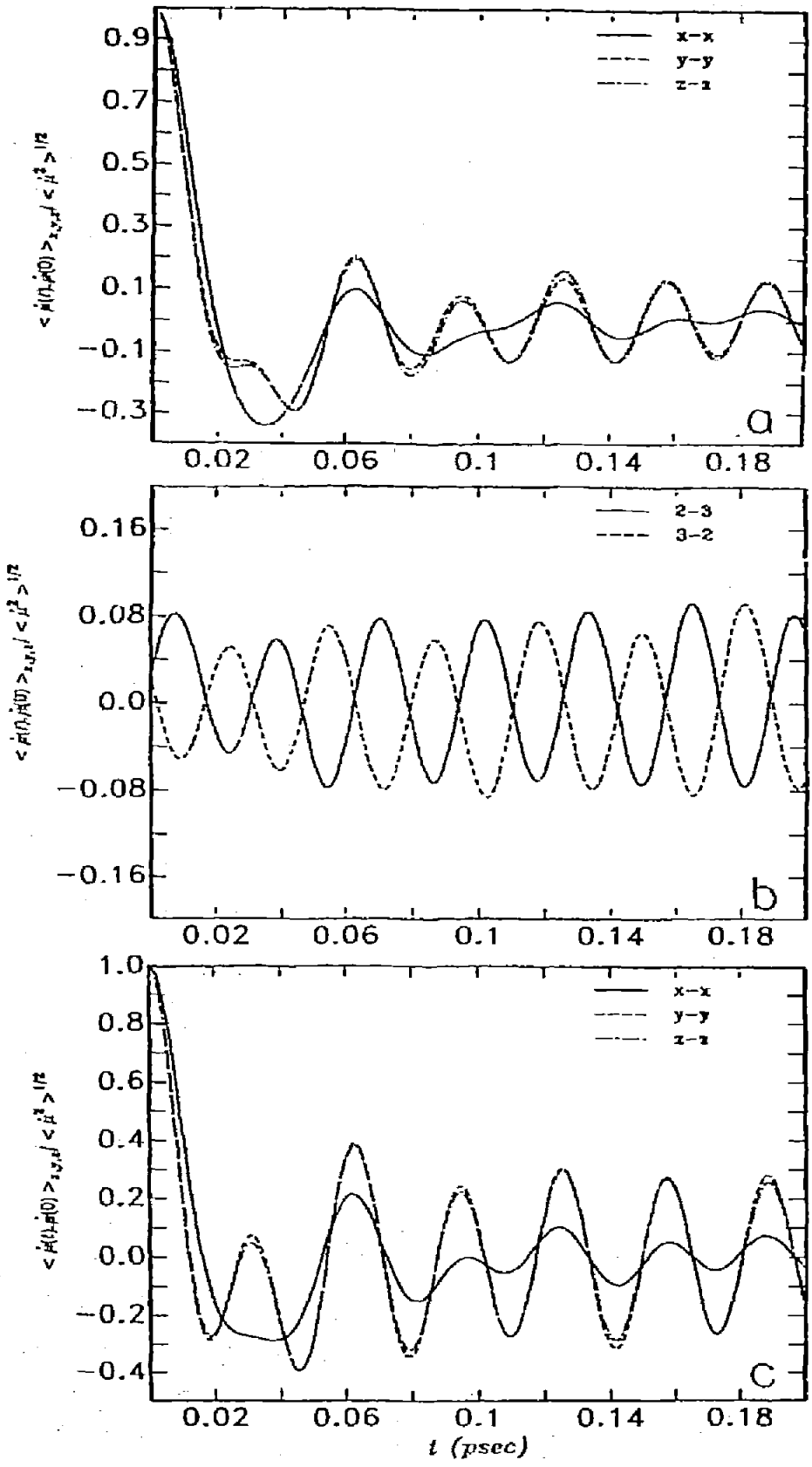
x-x
y-y
z-z
a
2-3
3-2
b
x-x
y-y
z-z
c
t (psec)

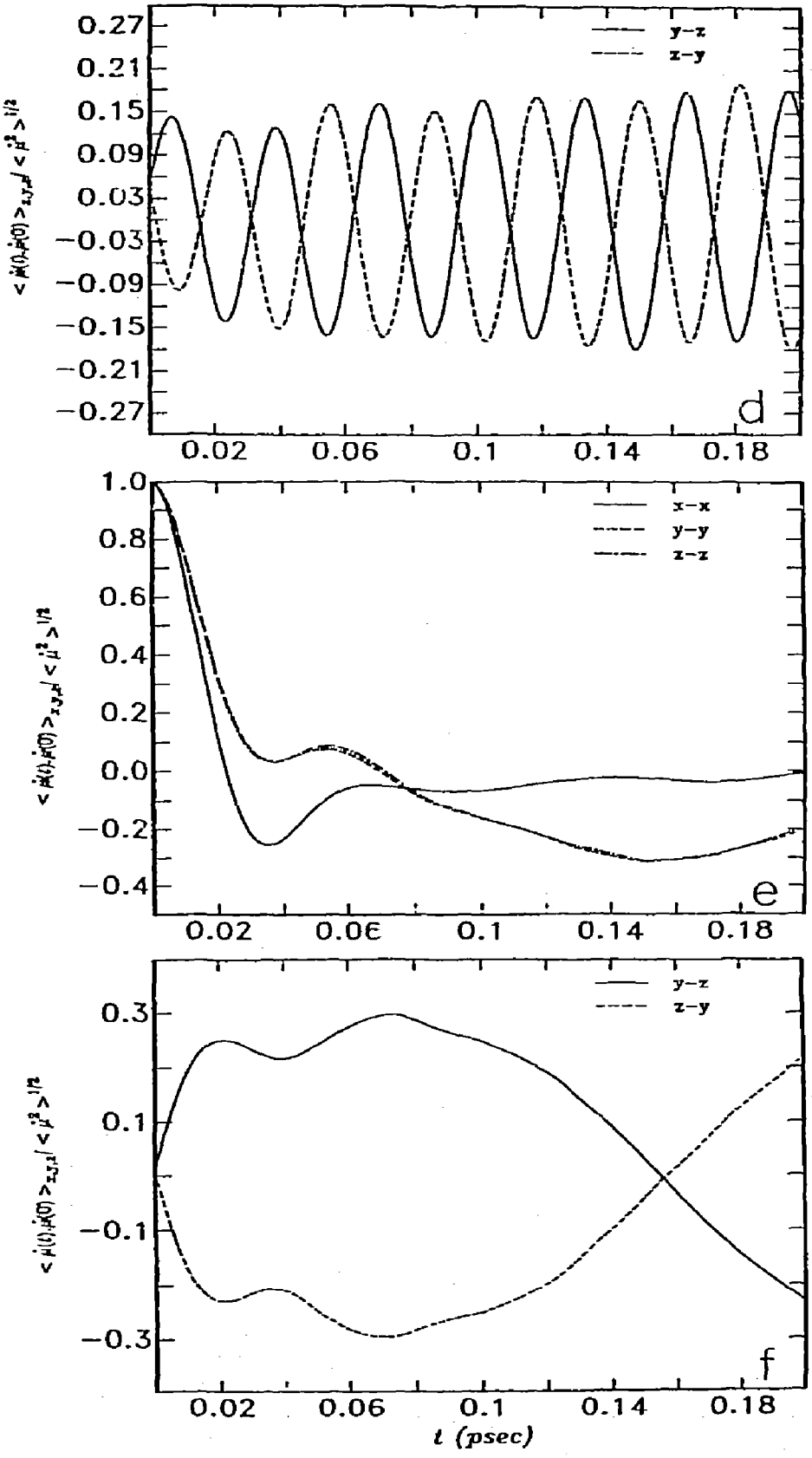
y–z
z–y
d
x–x
y–y
z–z
e
y–z
z–y
f
0.27
0.21
0.15
0.09
0.03
−0.03
−0.09
−0.15
−0.21
−0.27
1.0
0.8
0.6
0.4
0.2
0.0
−0.2
−0.4
0.3
0.1
−0.1
−0.3
0.02
0.06
0.1
0.14
0.18
t (psec)

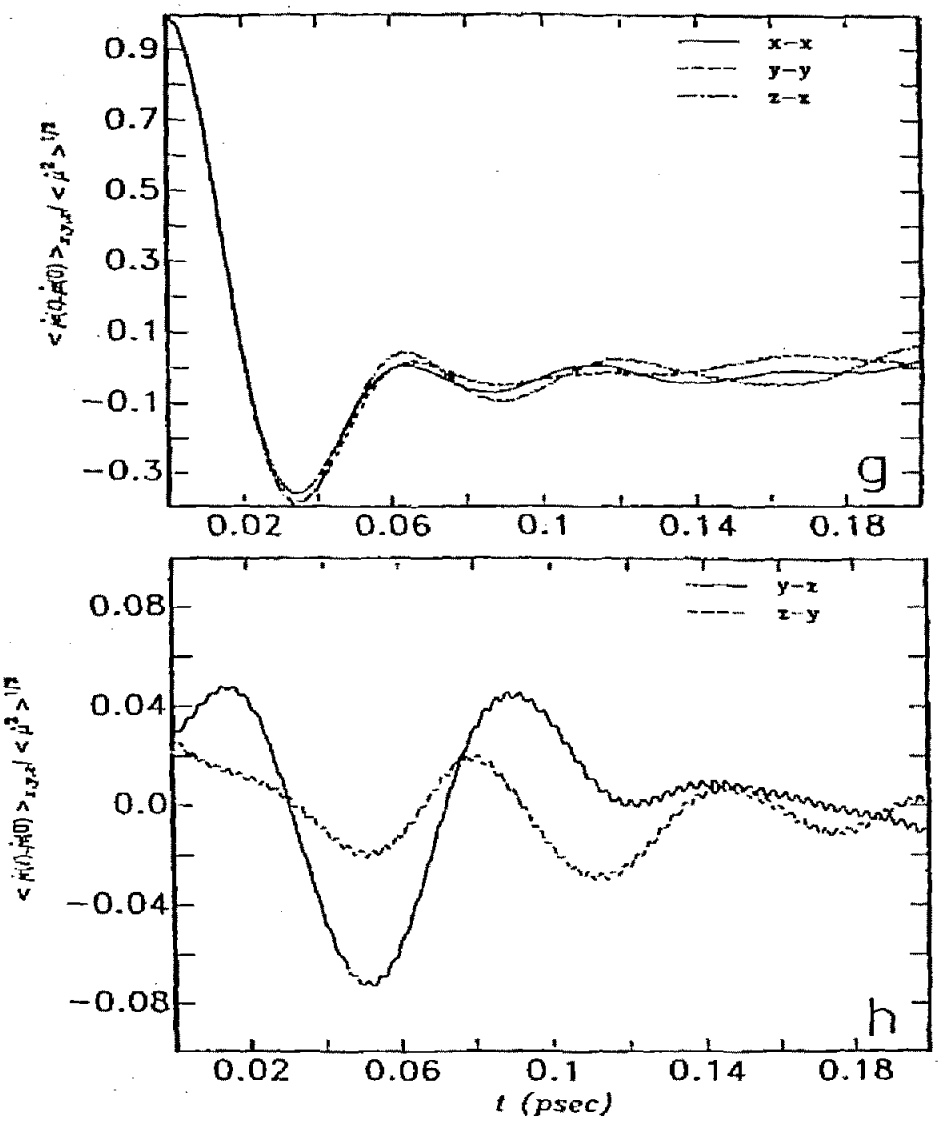

1. Figure (1). (a) Birefringence in the rotational velocity a.c.f. induced by a field of 10^{11} Hz. (b) (y, z) and (z, y) elements of the rotational velocity a.c.f. (c) Birefringence in the rotational velocity a.c.f. induced by a field of 10^{13} Hz. (d) (y, z) and (z, y) elements of the rotational velocity a.c.f. (e) Birefringence in the rotational velocity a.c.f. induced by a field of 10^{14} Hz. (f) (y, z) and (z, y) elements of the rotational velocity a.c.f. (g) Birefringence in the rotational velocity a.c.f. induced by a field of 10^{16} Hz. (h) (y, z) and (z, y) elements of the rotational velocity a.c.f.

Results and Discussion

The sequence of figures in this section illustrate the effect of increasing the ruby laser field frequency on the birefringence, as measured through the different time dependence of components of the rotational velocity and orientational autocorrelation functions. The first sequence (Fig. (1a)) illustrates the effect of increasing

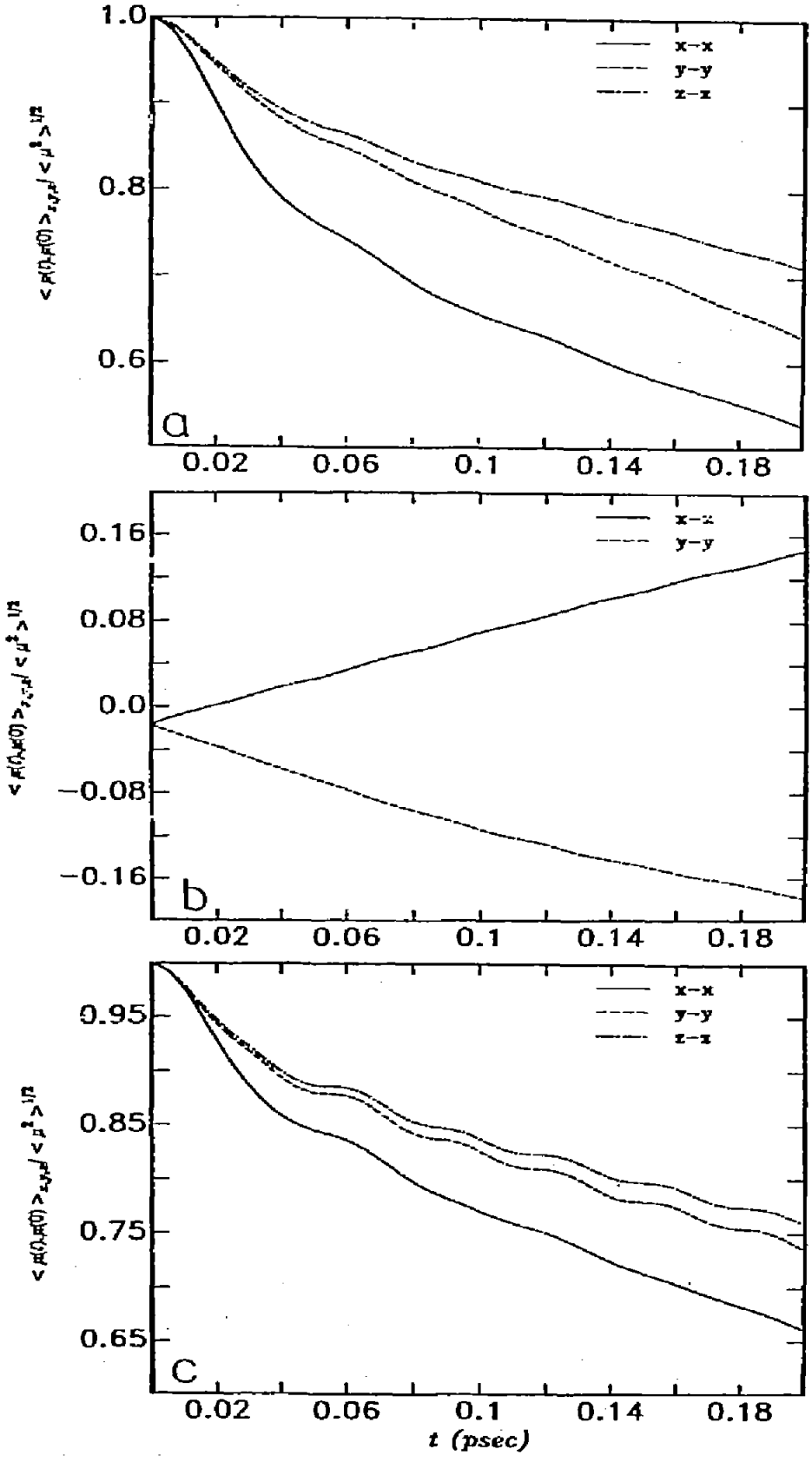
1.0
0.8
0.6
a
x–x
y–y
z–z
0.02
0.06
0.1
0.14
0.18
0.16
0.08
0.0
−0.08
−0.16
b
x–x
y–y
0.95
0.85
0.75
0.65
c
x–x
y–y
z–z
t (psec)

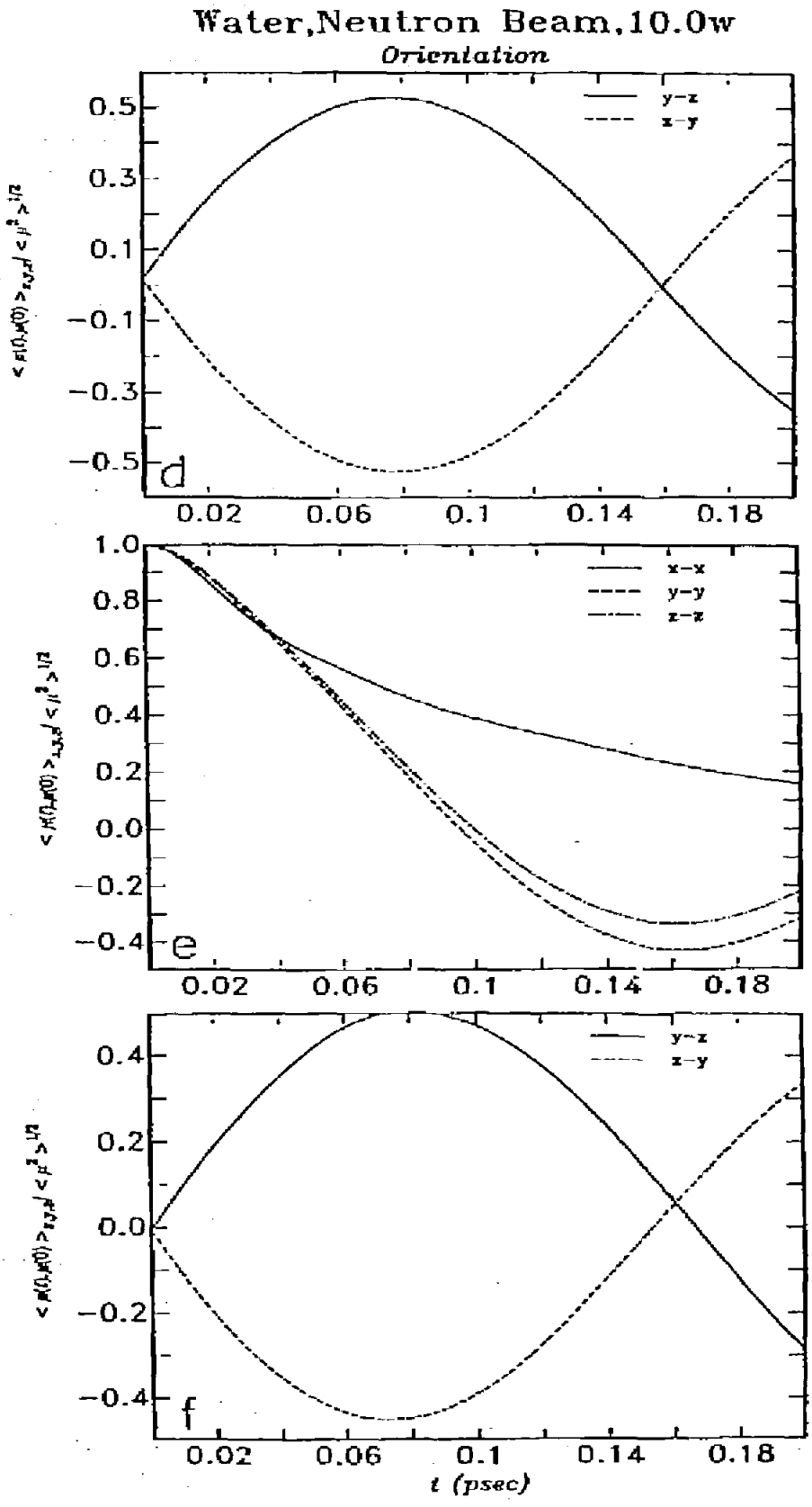
Water,Neutron Beam,10.0w
Orientation
y-z
x-y
d
x-x
y-y
z-z
e
y-z
x-y
f
t (psec)

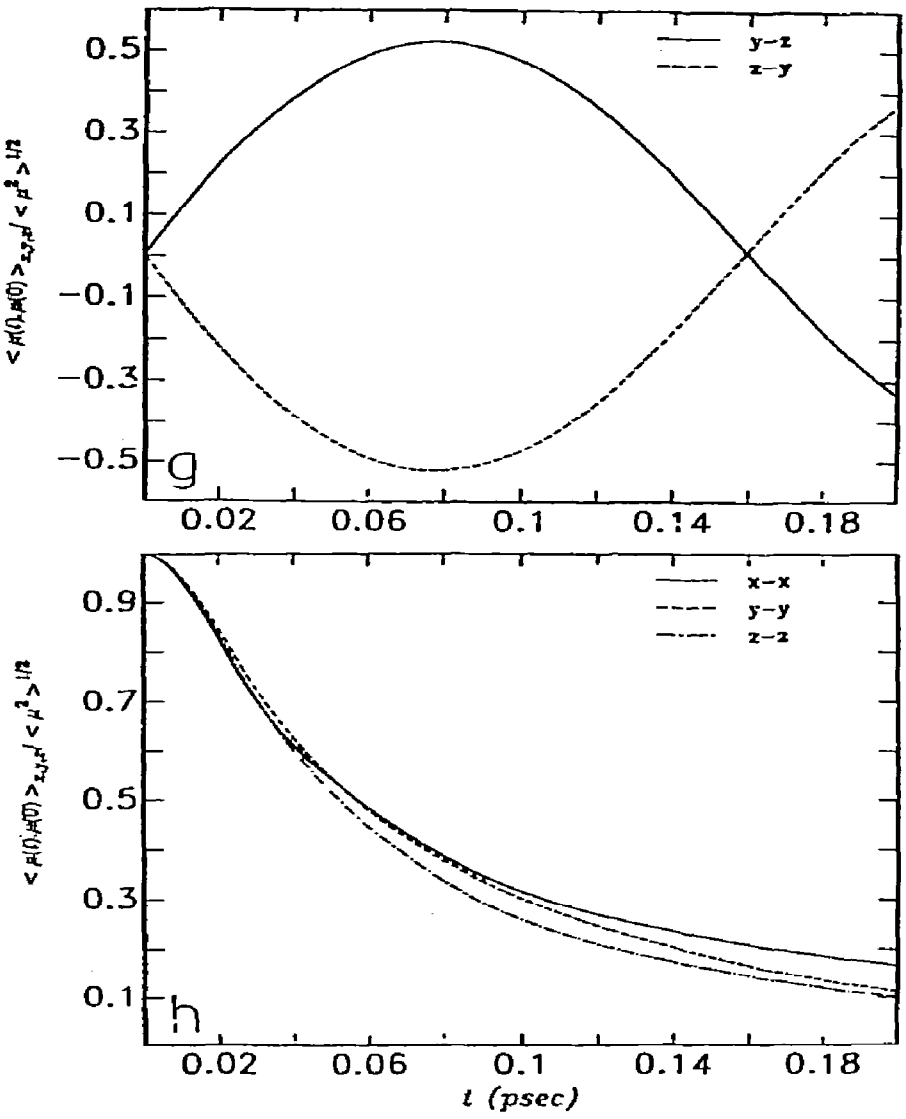

2. Figure (2). As for Fig. (1), orientational a.c.f. and off-diagonal elements.

the ruby laser frequency over orders of magnitude.At lower laser field frequencies (Fig. (1a)) the birefringence begins to appear superimposed on the field oscillations.The off-diagonal (y, z) and (z, y) elements of the rotational velocity a.c.f. appear in the laboratory frame of reference with the application of the giant ruby laser field over an interval of about 0.2 ps.This shows that it is feasible to use sub picosecond pulses of the giant ruby laser to induce birefringence in water.The fastest infra red detectors have response times in the nanosecond range.Therefore far infra-red dichroism and birefringence can be observed practically with trains of sub picosecond pulses of total duration in the nanosecond range.The presence simulation deals with the effect of one pulse of about 0.2 ps.

The amplitude of the off-diagonal elements is a measure of the birefringence and is dependent on the frequency of the ruby laser field. This is illustrated in Fig. (1). Although the off-diagonal elements cannot be directly observed experimentally they can be estimated by interpreting the ruby laser experiment with numerical computer simulation.

The equivalent of Fig. (1) for the orientational a.c.f. and off-diagonal elements are illustrated in Fig. (2), where the birefringence is clearly dependent on the field frequency.

In conclusion, the dispersion of laser induced far infra-red birefringence seems to be a new method of characterising optical saturation effects in molecular liquids.

Acknowledgement

I.B.M. is thanked for the award of a Visiting Professorship to MWE.

References

1. S. Wozniak, J. Chem. Phys., 85(8), 4217 (1986).
2. S. Kielich, "Dielectric and Related Molecular Processes", vol. 1, (Chem. Soc., London, 1972, Specialist Periodical Report).
3. W. T. Coffey, M. W. Evans, and P. Grigolini, "Molecular Diffusion", (Wiley / Interscience, New York, 1984).
4. "Memory Function Approaches to Stochastic Problems in Condensed Matter", ed. M. W. Evans, P. Grigolini, and G. Pastori-Parravicini, ser. ed. I. Prigogine and S. A. Rice, (Wiley / Interscience, New York, 1985).
5. M. W. Evans,G. J. Evans, W. T. Coffey and P. Grigolini, "Molecular Dynamics", (Wiley / Interscience, New York, 1982), chapter 2 on intense field effects.
6. G. Chantry "Submillimetre Spectroscopy", (Academic, New York, 1971)
7. M. W. Evans, Technical Report for Bruker Spectrospin, (1987).
8. M. W. Evans, Phys. Rev. Letters, 50, 371 (1983).